Progress In Electromagnetics Research C, Vol. 164, 51–57, 2026

PIER C

(Received 24 September 2025, Accepted 8 December 2025, Scheduled 27 December 2025)

Compact and Broadband CPW-to-RWG Transition Using 180° Phase Shifter

Yueh-Hsien Cheng, Chun-An Ko, Yi-Chih Lin, and Chun-Long Wang*

National Taiwan University of Science and Technology, Taipei 106335, Taiwan

ABSTRACT: In this paper, a compact and broadband 50-Ω coplanar waveguide-to-rectangular waveguide (CPW-to-RWG) transition using a 180° phase shifter is proposed. The frequency range, for which the reflection coefficient is smaller than −15 dB, covers the whole X-band (8.2 ∼ 12.4 GHz). In addition to the broadband performance, the transition occupies a small length of 7.37 mm. Furthermore, the characteristic impedance of the coplanar waveguide is 50 Ω, which conforms to the commonly used 50 Ω impedance of radio frequency systems. To further reduce the circuit size, a compact and broadband 50-Ω CPW-to-RWG transition using an inductance-compensated 180° phase shifter is proposed. The frequency range, for which the reflection coefficient is smaller than −15 dB, also covers the whole X-band (8.2 ∼ 12.4 GHz). Besides, the transition size is reduced from 7.37 mm to 6.55 mm, which is smaller than a quarter-wavelength. Furthermore, the characteristic impedance of the coplanar waveguide is of the nominal value of 50 Ω.

1. INTRODUCTION

In the past, many researchers have proposed various types of coplanar waveguide-to-rectangular waveguide (CPW-to-RWG) transitions [1–8]. In 1990, a CPW-to-RWG transition using the ridged waveguide was proposed by Ponchak and Simons [1]. Although this transition has broadband responses of low reflection coefficient and high transmission coefficient, the mechanical fabrication process used to implement the ridged waveguide is quite complicated and costly, in addition to the large size of the ridged waveguide. In 2009, the CPW-to-RWG transition using the ridged waveguide was successfully extended to W-band (75–110 GHz) [2]. Although the transition maintains the broadband response, the disadvantage of large size is still a problem.

To reduce the circuit size of the transition, CPW-to-RWG transitions using planar circuits were proposed [3–8]. Firstly, a CPW-to-RWG transition using the dipole slot antenna was proposed [3]. Although the structure is simple and as small as a quarter-wavelength, the broadband response is deteriorated. To enhance the bandwidth, a CPW-to-RWG transition using the rectangular patch was proposed [4]. Although the transition has a broadband response, a quarter-wavelength short-circuited rectangular waveguide is demanded, complicating the structure of the transition.

To prevent using the short-circuited rectangular waveguide, a CPW-to-RWG transition using the tapered fin-line was proposed [5]. The transition has a simple structure and broadband response, but the tapered fin-line will require a large circuit size. To reduce the circuit size, a CPW-to-RWG transition using the tapered slotline probe was proposed [6]. Although the circuit size can be reduced, an intermediate transition is required. Alternatively, a rectangular waveguide-to-rectangular waveguide transition using the quarter-wavelength probe was proposed to reduce the circuit size [7]. However, a quarter-wavelength substrate overhead is required. To eliminate the need for substrate overhead, a CPW-to-RWG transition using the inductance-compensated slotline was proposed [8]. The transition has a broadband response in addition to a small size of one-quarter-wavelength. However, the characteristic impedance of the coplanar waveguide is 117 Ω, which does not conform to the commonly used 50 Ω impedance of radio frequency systems.

All of the CPW-to-RWG transitions mentioned above [1–8] use a high value of the characteristic impedance of the coplanar waveguide, which does not conform to the nominal 50-Ω impedance of the radio frequency systems. To conform to the nominal 50-Ω impedance of radio frequency systems, a compact and broadband 50-Ω CPW-to-RWG transition using a 180° phase shifter is proposed. The bandwidth can cover the whole X-band (8.2–12.4 GHz), and the circuit size is as small as 7.37 mm, which is smaller than a quarter-wavelength. Furthermore, the characteristic impedance of the coplanar waveguide is 50 Ω, which conforms to the commonly used 50 Ω impedance of radio frequency systems. To further reduce the circuit size, a compact and broadband 50-Ω CPW-to-RWG transition using an inductance-compensated 180° phase shifter is proposed. The bandwidth can also cover the whole X-band (8.2–12.4 GHz), and the circuit size is as small as 6.44 mm, which is smaller than a quarter-wavelength. Furthermore, the characteristic impedance of the coplanar waveguide is 50 Ω, which conforms to the commonly used 50 Ω impedance of radio frequency systems.

* Corresponding author: Chun-Long Wang (clw@mail.ntust.edu.tw).

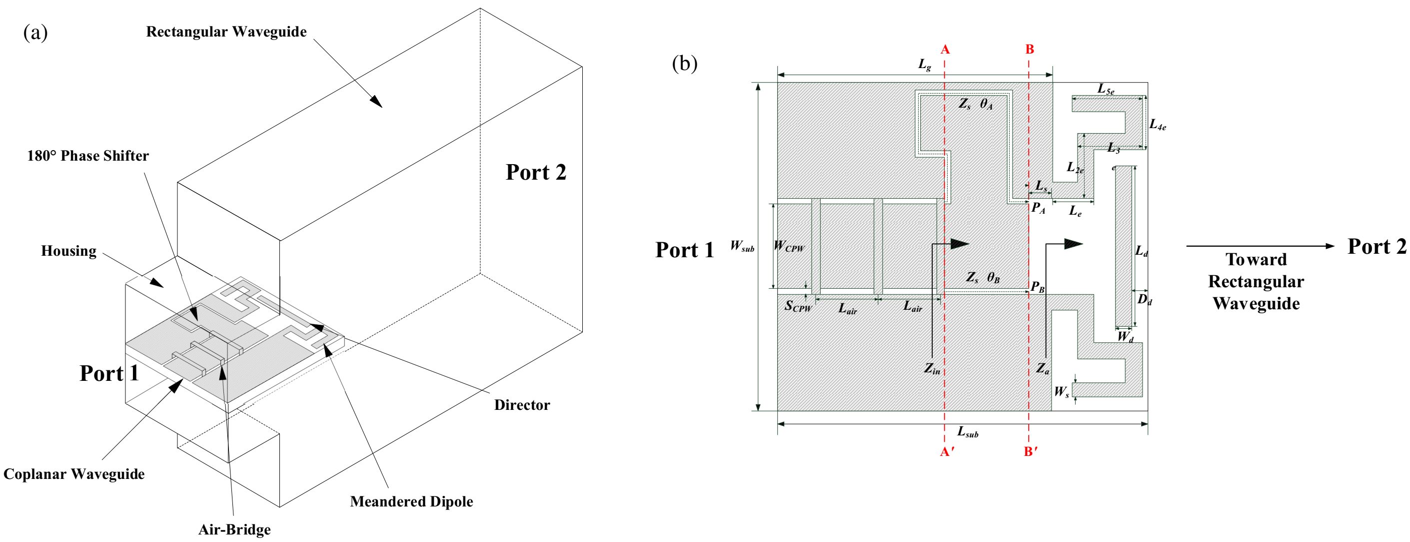

FIGURE 1. The structure of the 50-Ω CPW-to-RWG transition using the 180° phase shifter. (a) 3-D view. (b) Planar view.

2. COMPACT AND BROADBAND 50-Ω CPW-TO-RWG TRANSITION USING THE 180° PHASE SHIFTER

2.1. Topology

The 50-Ω CPW-to-RWG transition using a 180° phase shifter is depicted in Figure 1, where Figure 1(a) shows the 3-D view, and Figure 1(b) shows the planar view. As can be seen from the 3-D view shown in Figure 1(a), the transition consists of four parts, including a 50-Ω coplanar waveguide, a 180° phase shifter [9], a meandered dipole, and a rectangular waveguide. The 50-Ω coplanar waveguide is packaged with a housing dimension of 10.16 mm × 10.16 mm to eliminate the TE_{10} mode from propagating in the housing. Besides, three air-bridges are used to connect the ground planes of the coplanar waveguide to eliminate the coupled slotline mode from propagating in the housing. The 180° phase shifter is used to convert the coplanar waveguide mode into the slotline mode, which is then connected to the meandered dipole. Finally, the meandered dipole couples its energy into the rectangular waveguide, accomplishing the transition from the coplanar waveguide to the rectangular waveguide. The rectangular waveguide used is WR-90, which has a dimension of 22.86 mm × 10.16 mm, ensuring sole TE_{10} mode propagation in the X-band (8.2–12.4 GHz).

As can be seen from the planar view shown in Figure 1(b), the planar circuit consists of a 50-Ω coplanar waveguide, a 180° phase shifter, and a meandered dipole, which are fabricated on a Rogers®RO4003 substrate with a relative dielectric constant of 3.55, a loss tangent of 0.0027, and a thickness of 0.8 mm. To successfully couple the energy from the planar circuit to the rectangular waveguide, the planar circuit is placed in the middle of the rectangular waveguide, where the electric field of the TE_{10} mode is the strongest, as shown in Figure 1(a).

2.2. Equivalent Circuit

The equivalent circuit for the 50-Ω CPW-to-RWG transition using a 180° phase shifter shown in Figure 1(b) is depicted in Figure 2. As can be seen from Figure 2, the coplanar waveguide consists of one signal trace and two ground planes. The air-bridges are denoted by a simple electrical connection between the ground planes of the coplanar waveguide. The longer path P_A of the 180° phase shifter is represented by an ideal transmission line with a characteristic impedance Z_s and electrical length θ_A; the shorter path P_B of the 180° phase shifter is represented by an ideal transmission line with a characteristic impedance Z_s and electrical length θ_B. The input impedance looking into the meandered dipole is denoted by Z_a. As the ground planes of the coplanar waveguide are short-circuited, the relationship $V_1 = V_3$ must hold. As the load Z_a connects V_2 and V_4, the Kirchhoff relationship $V_2 - V_4 = Z_a I_2$ should be satisfied. As I_2 and I_4 flow in opposite directions, the relationship $I_2 = -I_4$ must be satisfied. By applying these criteria on the equivalent circuit, the input impedance looking into the 180° phase shifter, which is denoted by Z_{in}, can be expressed by (1).

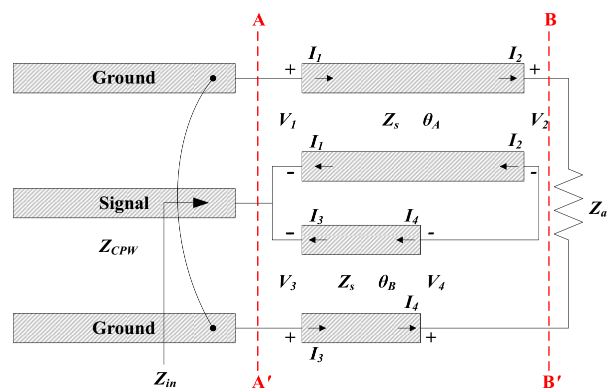

FIGURE 2. The equivalent circuit for the 50-Ω CPW-to-RWG transition using a 180° phase shifter.

$$
\begin{aligned}
Z_{in} &= \frac{V_3}{I_1 + I_3} \\
&= \frac{Z_a \cos\theta_A \cos\theta_B + jZ_s \sin(\theta_A + \theta_B)}{2\cos(\theta_A + \theta_B) - 2 + j(Z_a/Z_s)\sin(\theta_A + \theta_B)}
\end{aligned}
\quad (1)
$$

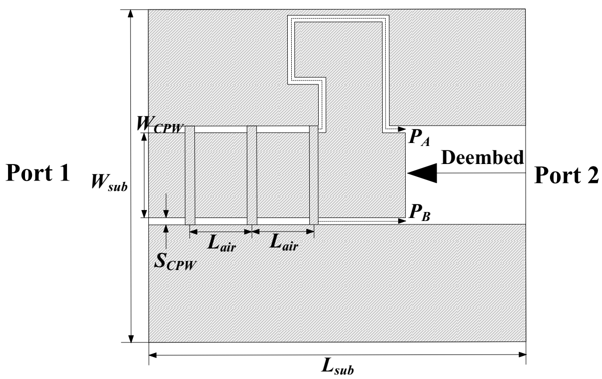

FIGURE 3. The structure of the 180° phase shifter.

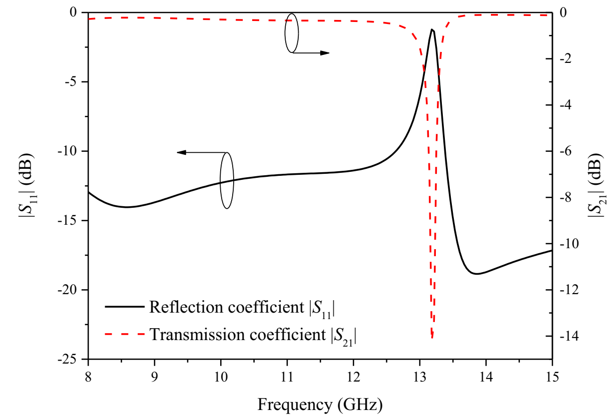

FIGURE 4. The frequency responses of the reflection and transmission coefficients for the 180° phase shifter.

As can be observed from (1), when the denominator of the input impedance Z_{in} is zero, the value of the input impedance Z_{in} will be infinite, where there will be an undesirable resonance. By setting the real and imaginary parts of the denominator of the input impedance Z_{in} equal to zero, the relationship $\theta_A(f_r) + \theta_B(f_r) = 2\pi$ must be satisfied at the resonance frequency f_r. This can be further rewritten as (2) where $\theta_A(f_0)$ denotes the electrical length of the longer path P_A of the 180° phase shifter at the center frequency f_0, and $\theta_B(f_0)$ denotes the electrical length of the shorter path P_B of the 180° phase shifter at the center frequency f_0.

$$\frac{f_r}{f_0} \times \theta_A(f_0) + \frac{f_r}{f_0} \times \theta_B(f_0) = 2\pi \tag{2}$$

Besides, reconsidering the equivalent circuit shown in Figure 2, since the 180° phase shifter is designed to have a 180° electrical length difference between the longer path P_A and shorter path P_B at the center frequency f_0, the relationship between the longer path P_A and shorter path P_B shown in (3) must hold.

$$\theta_A(f_0) - \theta_B(f_0) = \pi \tag{3}$$

The resonance frequency f_r is the inherent characteristic of the 180° phase shifter. It is inevitable and should be pushed out of the operational band (8.2–12.4 GHz) of the transition so that the transition performance will not be degraded. To prevent affecting the transition performance, the value of the undesirable resonance frequency f_r is deliberately chosen to be 13.63 GHz, which falls outside the operational band (8.2–12.4 GHz) of the transition. Given the value of the center frequency $f_0 = 12.2$ GHz and the value of the undesirable resonance frequency $f_r = 13.63$ GHz, the electrical length $\theta_A(f_0)$ of the longer path P_A and the electrical length $\theta_B(f_0)$ of the shorter path P_B at the center frequency f_0 can be calculated through (2) and (3). Their values are $\theta_A(f_0) = 251°$ and $\theta_B(f_0) = 71°$.

2.3. Implementation of the 180° Phase Shifter

Reconsidering the planar circuit shown in Figure 1(b), the 50-Ω coplanar waveguide is implemented with the dimensions of $W_{CPW} = 2.6$ mm and $S_{CPW} = 0.2$ mm. As $S_{CPW} = 0.2$ mm, the characteristic impedances Z_s of the longer path P_A and shorter path P_B will be 100 Ω. As the electrical length of the longer path P_A is $\theta_A(f_0) = 251°$, it can be implemented with a path length of 11.6 mm. As the electrical length of the shorter path P_B is $\theta_B(f_0) = 71°$, it can be implemented with a path length of 2.6 mm. The height, width, and length of the air-bridges are 0.4 mm, 0.3 mm, and 2.6 mm, respectively. The distance L_{air} between adjacent air-bridges is 1.9 mm. The structure of the 180° phase shifter is redrawn in Figure 3 for clarity, where $L_{sub} = 11.42$ mm and $W_{sub} = 10.16$ mm. To obtain the frequency responses of the reflection and transmission coefficients of the 180° phase shifter, the structure of the 180° phase shifter shown in Figure 3 is simulated by using the Ansoft HFSS. The frequency responses of reflection and transmission coefficients are shown in Figure 4. As can be seen from Figure 4, there is an undesirable resonance frequency at 13.18 GHz, which is slightly lower than the designed value of 13.63 GHz. The reduction in the resonance frequency is attributed to the meandering effect of the longer path P_A, which will increase the effective electrical length of the longer path P_A. As a result, the resonance frequency will be reduced. Even so, the resonance frequency still falls outside of the X-band (8.2–12.4 GHz), so that the performance of the transition will not deteriorate.

2.4. Implementation of the Meandered Dipole

Reconsidering the planar circuit of the CPW-to-RWG transition using the 180° phase shifter shown in Figure 1(b) to achieve a good transition performance, the input impedance of the meandered dipole Z_a should be matched to the output impedance of the 180° phase shifter, which means that they should be complex conjugate with each other. By simulating the 180° phase shifter shown in Figure 3 with the Ansoft HFSS and taking the complex conjugate value of the reflection coefficient S_{22} at the output port 2, the desired frequency response of the input impedance Z_a of the meandered dipole can be acquired as shown in Figure 5.

The structure of the meandered dipole is redrawn in Figure 6 for clarity. To achieve the desired frequency response of the input impedance Z_a of the meandered dipole shown in Figure 5, the dimensions of the meandered dipole and the director shown

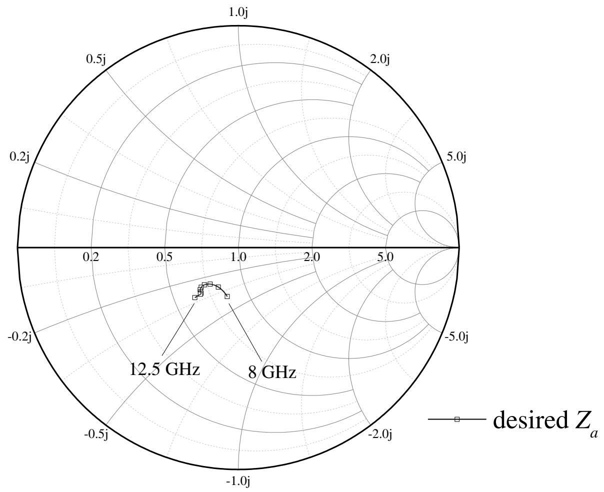

FIGURE 5. The desired frequency response of the input impedance Z_a of the meandered dipole.

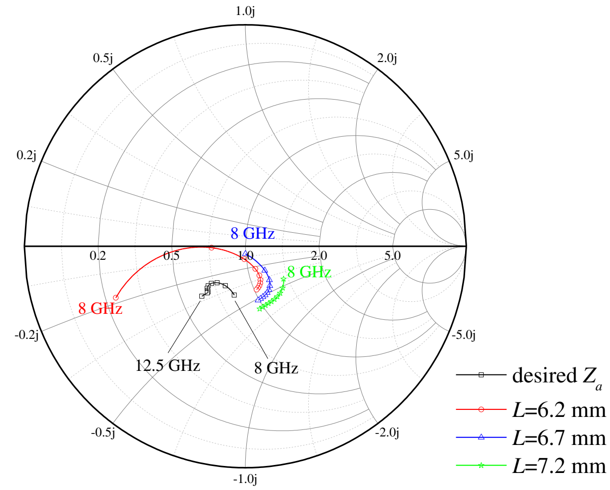

FIGURE 7. The frequency responses of the input impedance Z_a for various lengths of the meandered dipole.

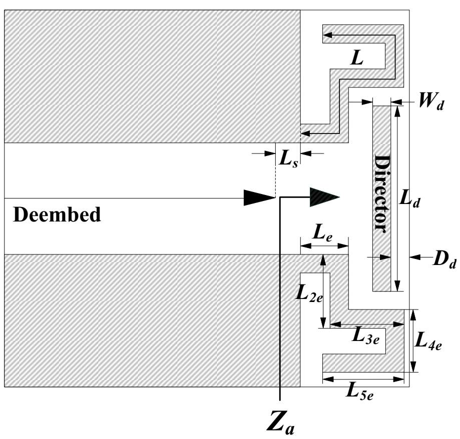

FIGURE 6. The structure of the meandered dipole.

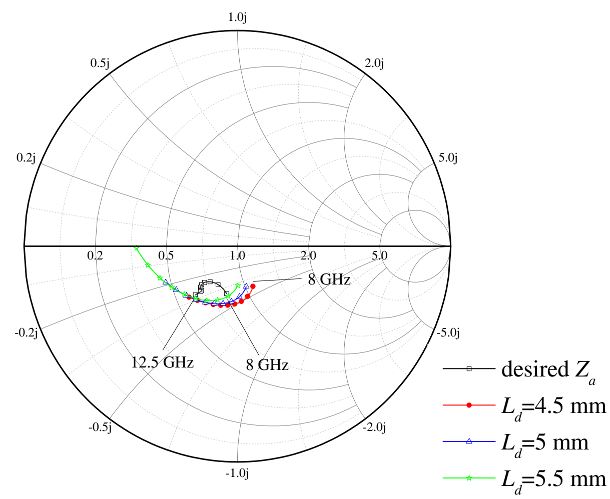

FIGURE 8. The frequency responses of the input impedance Z_a for various lengths of the director.

in Figure 6 should be properly designed. At first, the director is removed to determine the length of the meandered dipole. The meandered dipole without the director shown in Figure 6 is simulated by using the Ansoft HFSS as the length of the meandered dipole is varied from 6.2 mm to 7.2 mm. The frequency responses of the input impedance Z_a for various lengths of the meandered dipole are shown in Figure 7. As can be seen from Figure 7, the length of the meandered dipole is determined to be 7.2 mm as the frequency response of the input impedance Z_a is compact. With the length of the meandered dipole set as 7.2 mm, the structure of the meandered dipole with the director shown in Figure 6 is simulated with the Ansoft HFSS as the length of the director L_d is varied from 4.5 mm to 5.5 mm. The frequency responses of the input impedance Z_a for various lengths of the director are shown in Figure 8. As can be seen from Figure 8, the length of the director is determined to be 4.5 mm, as the frequency response of the input impedance Z_a is compact and close to the desired frequency response of the input impedance Z_a.

2.5. Performance of the Full Transition

By integrating the 180° phase shifter shown in Figure 3 and the meandered dipole shown in Figure 6, the CPW-to-RWG transition using a 180° phase shifter can be formed as shown in Figure 1(b). The dimensions for the CPW-to-RWG transition using a 180° phase shifter are listed in Table 1. The CPW-to-RWG transition using the 180° phase shifter shown in Figure 1(b), along with the dimensions listed in Table 1, is simulated by using the Ansoft HFSS, and the frequency responses of the reflection and transmission coefficients are shown in Figure 9. As can be seen from Figure 9, the frequency range for which the reflection coefficient is smaller than -15 dB covers from 8.21 GHz to 12.9 GHz, almost encompassing the whole X-band (8.2–12.4 GHz), and the transmission coefficient is larger than -0.244 dB. Besides, the length of the transition is as small as 7.37 mm. Furthermore, the characteristic impedance of the coplanar waveguide is of the nominal value of 50 Ω.

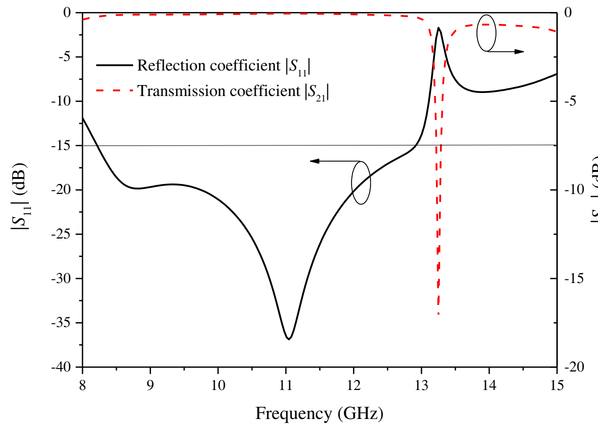

FIGURE 9. The frequency responses of the reflection and transmission coefficients for the CPW-to-RWG transition using the 180° phase shifter.

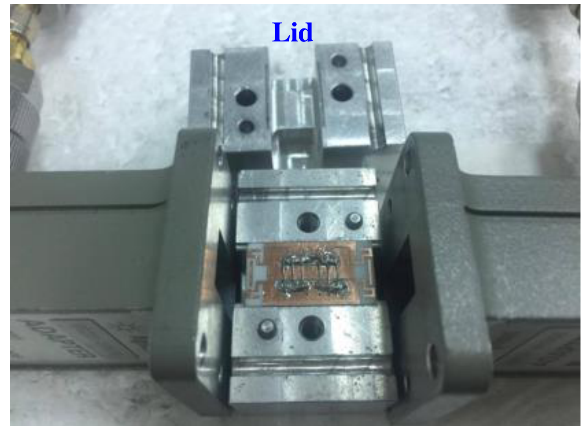

FIGURE 10. The real circuit for the back-to-back CPW-to-RWG transition using the 180° phase shifter.

TABLE 1. The dimensions for the CPW-to-RWG transition using the 180° phase shifter.

W_{sub}	W_{CPW}	W_s	W_d	S_{CPW}	L_{sub}	L_s	L_g	L_d	L_e
10.16	2.6	0.5	0.5	0.2	11.42	0.7	8.47	5	1.3
L_{e2}	L_{e3}	L_{e4}	L_{e5}	L_{air}	D_d	P_A	P_B	Unit	
2	2	1.7	2.2	1.9	0.5	11.6	2.6	mm	

2.6. Verification

In order to verify the simulation results, two CPW-to-RWG transitions using the 180° phase shifter are connected back-to-back and fabricated as shown in Figure 10. During the measurement, the lid shown in Figure 10 is placed on top of the back-to-back transition so that the back-to-back transition forms a closed structure. The back-to-back transition shown in Figure 10 is then measured with the Agilent N5242A PNA after the PNA is calibrated with the waveguide calibration kit X11644A STL (Short-Through-Line). The measured frequency responses of the reflection and transmission coefficients are shown in Figure 11. For comparison, the back-to-back transition is also simulated with Ansoft HFSS, and the simulated frequency responses of the reflection and transmission coefficients are also shown in Figure 11. As can be seen from Figure 11, the simulation and measurement results agree well except for some frequency shifts, which are attributed to the soldering effect of the air-bridges.

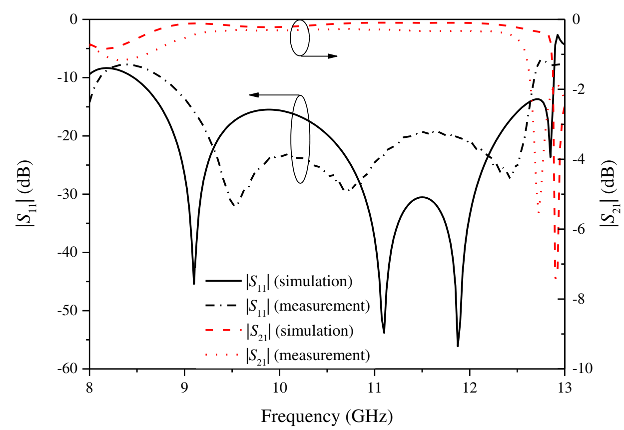

FIGURE 11. Comparison between the simulated and measured frequency responses of the reflection and transmission coefficients for the back-to-back CPW-to-RWG transition using the 180° phase shifter.

3. COMPACT AND BROADBAND 50-Ω CPW-TO-RWG TRANSITION USING THE INDUCTANCE-COMPENSATED 180° PHASE SHIFTER

3.1. Topology

To further reduce the size of the CPW-to-RWG transition using the 180° phase shifter shown in Figure 1(b), the 180° phase shifter is replaced with an inductance-compensated 180° phase shifter. The resulting CPW-to-RWG transition using the inductance-compensated 180° phase shifter is shown in Figure 12. As can be seen from Figure 12, the longer path P_A of the 180° phase shifter is miniaturized through the inductance-compensated technique [8], while the shorter path P_B of the 180° phase shifter remains the same as listed in Table 1. The dimensions for the CPW-to-RWG transition using the inductance-compensated 180° phase shifter are listed in Table 2. The structure of the CPW-to-RWG transition using the inductance-compensated 180° phase shifter shown in Figure 12, along with the dimensions listed in Table 2, is simulated by using the Ansoft HFSS, and the frequency responses of the reflection and transmission coefficients are shown in Figure 13. As can be seen from Figure 13, the frequency range for which the reflection coefficient is smaller than -15 dB covers from 8.22 GHz to 12.83 GHz, almost encompassing the whole X-

TABLE 2. The dimensions for the CPW-to-RWG transition using the inductance-compensated 180° phase shifter.

W_{sub}	W_{CPW}	W_s	W_d	W_{s1}	W_{s2}	S_{CPW}	L_{sub}	L_s	L_g	L_d
10.16	2.6	0.5	0.5	0.2	0.2	0.2	11.42	0.7	8.47	5
L_e	L_{e2}	L_{e3}	L_{e4}	L_{e5}	L_{air}	L_{sp}	D_d	P_B	Unit	
1.3	2	2	1.7	2.2	1.9	0.62	0.5	2.6	mm	

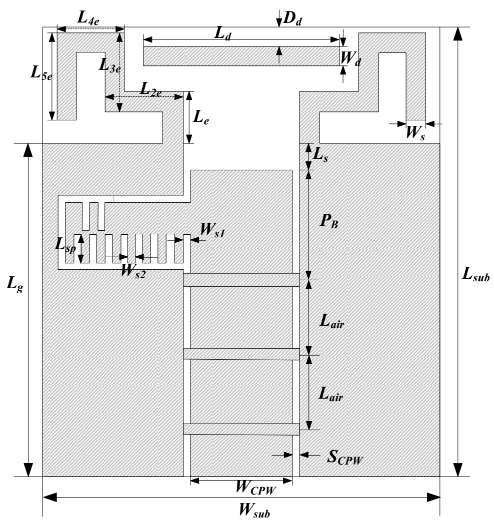

FIGURE 12. The structure of the 50-Ω CPW-to-RWG transition using the inductance-compensated 180° phase shifter.

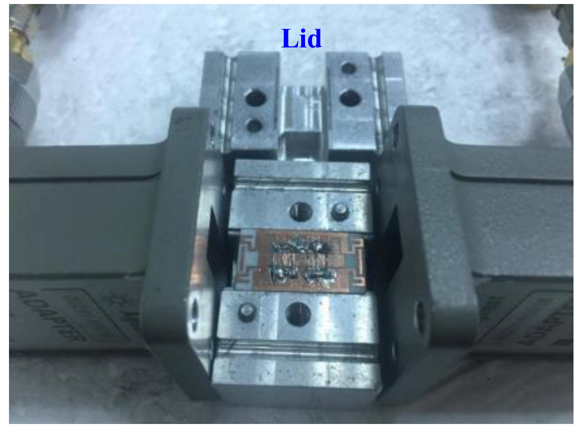

FIGURE 14. The real circuit for the back-to-back CPW-to-RWG transition using the inductance-compensated 180° phase shifter.

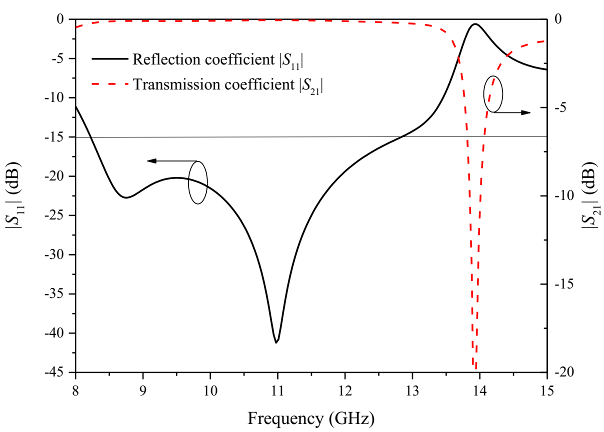

FIGURE 13. The frequency responses of the reflection and transmission coefficients for the CPW-to-RWG transition using the inductance-compensated 180° phase shifter.

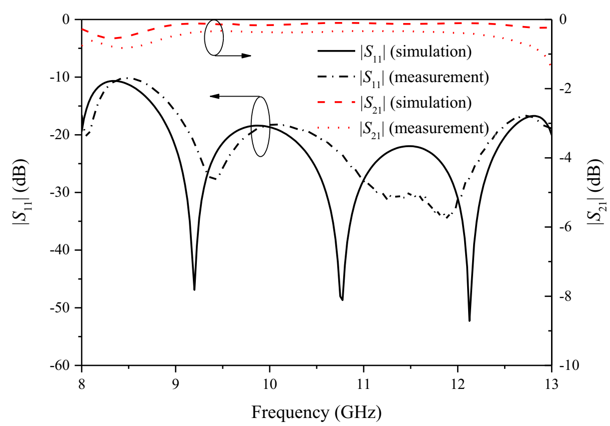

FIGURE 15. Comparison between the simulated and measured frequency responses of the reflection and transmission coefficients for the back-to-back CPW-to-RWG transition using the inductance-compensated 180° phase shifter.

band (8.2–12.4 GHz), and the transmission coefficient is larger than -0.22 dB. Besides, the length of the transition is as small as 6.55 mm, which is smaller than a quarter-wavelength. Furthermore, the characteristic impedance of the coplanar waveguide is of the nominal value of 50 Ω.

3.2. Verification

To verify the simulation results, two CPW-to-RWG transitions using the inductance-compensated 180° phase shifter are connected back-to-back and fabricated as shown in Figure 14. During the measurement, the lid shown in Figure 14 is placed on top of the back-to-back transition so that the back-to-back transition forms a closed structure. The back-to-back transition shown in Figure 14 is then measured with the Agilent N5242A PNA after the PNA is calibrated with the waveguide calibration kit X11644A STL (Short-Through-Line). The measured frequency responses of the reflection and transmission coefficients are shown in Figure 15. For comparison, the back-to-back transition is also simulated with Ansoft HFSS, and the simulated frequency responses of the reflection and transmission coefficients are also shown in Figure 15. As can be seen from Figure 15, the simulation and measurement results agree well except for some frequency shifts, which are attributed to the soldering effect of the air-bridges.

TABLE 3. Comparison between the performances of various compact and broadband transitions.

Transition Type	-15-dB Fractional Bandwidth (%)	Circuit Size (mm)	Characteristic Impedance (Ω)	$\lvert S_{21}\rvert$ (dB)
Dipole slot [3]	22.85	12.00	75	-0.17
Fin-line taper [5]	40.78	15.00	57	-0.13
Slotline probe [6]	40.00	13.97	109	-0.33
Inductance-compensated slotline [8]	38.06	9.40	115	-0.21
180° phase shifter	45.50	7.37	50	-0.24
Inductance-compensated 180° phase shifter	44.76	6.55	50	-0.22

4. CONCLUSION

In this paper, the compact and broadband 50-Ω CPW-to-RWG transition using a 180° phase shifter is proposed. By deliberately pushing the resonance frequency of the 180° phase shifter out of the X-band (8.2–12.4 GHz), the frequency range for which the reflection coefficient is smaller than -15 dB can cover from 8.21 GHz to 12.9 GHz, almost encompassing the whole X-band (8.2–12.4 GHz), and the transmission coefficient is larger than -0.244 dB for a single transition. In addition to the broadband performance, the transition occupies a small length of 7.37 mm. Furthermore, the characteristic impedance of the coplanar waveguide is 50 Ω, which conforms to the commonly used 50-Ω impedance of the radio frequency systems. To further reduce the circuit size, a compact and broadband 50-Ω CPW-to-RWG transition using the inductance-compensated 180° phase shifter is proposed. The frequency range for which the reflection coefficient is smaller than -15 dB covers from 8.22 GHz to 12.83 GHz, almost encompassing the whole X-band (8.2–12.4 GHz), and the transmission coefficient is larger than -0.22 dB for a single transition. Besides, the length of the transition is as small as 6.55 mm, which is smaller than a quarter-wavelength. Furthermore, the characteristic impedance of the coplanar waveguide is of the nominal value of 50 Ω. To verify the simulation results, two back-to-back 50-Ω CPW-to-RWG transitions are fabricated and measured. The simulation and measurement results of the back-to-back transitions agree well except for some frequency shifts, which are caused by the soldering effect of the air-bridges. Table 3 summarizes the performance of some compact and broadband transitions. As can be seen from Table 3, the CPW-to-RWG transition using the inductance-compensated 180° phase shifter has the smallest size of 6.55 mm and a broad bandwidth of 44.76%. Furthermore, the characteristic impedance of the coplanar waveguide is 50 Ω, which is compatible to the nominal 50 Ω impedance of radio frequency systems.

ACKNOWLEDGEMENT

This work was supported in part by the National Science and Technology Council, Taiwan, under Grant NSTC 114-2221-E-011-075. The authors would like to thank Wireless Communications & Applied Electromagnetic LAB, National Taiwan University of Science and Technology, for providing the simulation environment of Ansoft® HFSS V.13 and the measurement instruments.

REFERENCES

[1] Ponchak, G. E. and R. N. Simons, "A new rectangular waveguide to coplanar waveguide transition," in *IEEE International Digest on Microwave Symposium*, Vol. 1, 491–492, Dallas, TX, USA, 1990.

[2] Shireen, R., S. Shi, P. Yao, C. A. Schuetz, J. Macario, and D. W. Prather, "CPW to rectangular waveguide transition on an $LiNbO_3$ substrate," *IEEE Transactions on Microwave Theory and Techniques*, Vol. 57, No. 6, 1494–1499, Jun. 2009.

[3] Fang, R.-Y., C.-T. Wang, and C.-L. Wang, "A direct CPW-to-rectangular waveguide transition using a dipole slot antenna," in *2009 European Microwave Conference (EuMC)*, 157–160, Rome, Italy, 2009.

[4] Dong, Y., T. K. Johansen, V. Zhurbenko, and P. J. Hanberg, "Rectangular waveguide-to-coplanar waveguide transitions at U-band using E-plane probe and wire bonding," in *2016 46th European Microwave Conference (EuMC)*, 5–8, London, UK, 2016.

[5] Mottonen, V. S., "Wideband coplanar waveguide-to-rectangular waveguide transition using fin-line taper," *IEEE Microwave and Wireless Components Letters*, Vol. 15, No. 2, 119–121, Feb. 2005.

[6] Lin, T.-H. and R.-B. Wu, "CPW to waveguide transition with tapered slotline probe," *IEEE Microwave and Wireless Components Letters*, Vol. 11, No. 7, 314–316, Jul. 2001.

[7] Mottonen, V. S. and A. V. Raisanen, "Novel wide-band coplanar waveguide-to-rectangular waveguide transition," *IEEE Transactions on Microwave Theory and Techniques*, Vol. 52, No. 8, 1836–1842, Aug. 2004.

[8] Fang, R.-Y. and C.-L. Wang, "Miniaturized coplanar waveguide to rectangular waveguide transition using inductance-compensated slotline," *IEEE Transactions on Components, Packaging and Manufacturing Technology*, Vol. 2, No. 10, 1666–1671, Oct. 2012.

[9] Ma, K.-P., Y. Qian, and T. Itoh, "Analysis and applications of a new CPW-slotline transition," *IEEE Transactions on Microwave Theory and Techniques*, Vol. 47, No. 4, 426–432, Apr. 1999.